Journal of Maps

ISSN: (Print) 1744-5647 (Online) Journal homepage: https://www.tandfonline.com/loi/tjom20

Surface ruptures following the 26 December 2018, Mw 4.9, Mt. Etna earthquake, Sicily (Italy)

EMERGEO Working Group (Etna 2018)

Riccardo Civico, Stefano Pucci, Rosa Nappi, Raffaele Azzaro, Fabio Villani, Daniela Pantosti, Francesca R. Cinti, Luca Pizzimenti, Stefano Branca, Carlo Alberto Brunori, Marco Caciagli, Massimo Cantarero, Luigi Cucci, Salvatore D'Amico, Emanuela De Beni, Paolo Marco De Martini, Maria Teresa Mariucci, Paola Montone, Rosella Nave, Tullio Ricci, Vincenzo Sapia, Alessandra Smedile, Gabriele Tarabusi, Roberto Vallone & Alessandra Venuti

To cite this article: Riccardo Civico, Stefano Pucci, Rosa Nappi, Raffaele Azzaro, Fabio Villani, Daniela Pantosti, Francesca R. Cinti, Luca Pizzimenti, Stefano Branca, Carlo Alberto Brunori, Marco Caciagli, Massimo Cantarero, Luigi Cucci, Salvatore D'Amico, Emanuela De Beni, Paolo Marco De Martini, Maria Teresa Mariucci, Paola Montone, Rosella Nave, Tullio Ricci, Vincenzo Sapia, Alessandra Smedile, Gabriele Tarabusi, Roberto Vallone & Alessandra Venuti (2019) Surface ruptures following the 26 December 2018, Mw 4.9, Mt. Etna earthquake, Sicily (Italy), Journal of Maps, 15:2, 831-837, DOI: 10.1080/17445647.2019.1683476

To link to this article: https://doi.org/10.1080/17445647.2019.1683476

Published online: 01 Nov 2019.

JOURNAL OF MAPS
2019, VOL. 15, NO. 2, 831–837
https://doi.org/10.1080/17445647.2019.1683476

Science

OPEN ACCESS Check for updates

Surface ruptures following the 26 December 2018, Mw 4.9, Mt. Etna earthquake, Sicily (Italy)
EMERGEO Working Group (Etna 2018)

Riccardo Civico, Stefano Pucci, Rosa Nappi, Raffaele Azzaro, Fabio Villani, Daniela Pantosti, Francesca R. Cinti, Luca Pizzimenti, Stefano Branca, Carlo Alberto Brunori, Marco Caciagli, Massimo Cantarero, Luigi Cucci, Salvatore D'Amico, Emanuela De Beni, Paolo Marco De Martini, Maria Teresa Mariucci, Paola Montone, Rosella Nave, Tullio Ricci, Vincenzo Sapia, Alessandra Smedile, Gabriele Tarabusi, Roberto Vallone and Alessandra Venuti

Istituto Nazionale di Geofisica e Vulcanologia, Italy

ABSTRACT
We present a 1:10,000 scale map of the coseismic surface ruptures following the 26 December 2018 Mw 4.9 earthquake that struck the eastern flank of Mt. Etna volcano (southern Italy). Detailed rupture mapping is based on extensive field surveys in the epicentral region. Despite the small size of the event, we were able to document surface faulting for about 8 km along the trace of the NNW-trending active Fiandaca Fault, belonging to the Timpe tectonic system in the eastern flank of the volcano. The mapped ruptures are characterized in most cases by perceivable opening and by a dominant right-oblique sense of slip, with an average slip of about 0.09 m and a peak value of 0.35 m. It is also noteworthy that the ruptures vary significantly in their kinematic expression, denoting locally high degree of complexity of the surface faulting.

ARTICLE HISTORY
Received 2 September 2019
Accepted 18 October 2019

KEYWORDS
Surface faulting; coseismic ruptures; geological prompt survey; earthquake; 2018 Mt. Etna volcano seismic sequence; southern Italy

1. Introduction

On 26 December 2018 (02:19 UTC), a Mw 4.9 (ML 4.8) earthquake located at a depth of less than 1 km (http://cnt.rm.ingv.it/en/event/21285011), struck the south-eastern flank of Mt. Etna volcano (southern Italy), producing severe damage in the towns and villages of the area (QUEST Working Group, 2019), 10 injured and more than 1100 homeless. This earthquake occurred 5 km NW of the town of Acireale (Figure 1) and has been followed by an intense seismic swarm (ca. 250 events with ML < 3 until the end of February 2019) accompanying the eruptive phase of Mt. Etna which started on 23 December 2018. While the seismic swarm was associated with a dyke intrusion in the upper part of Etna, inducing significant deformation of the volcanic edifice (Bonforte, Guglielmino, & Puglisi, 2019; De Novellis et al., 2019), the 26 December Mw 4.9 earthquake was generated by the Fiandaca fault (FF), probably influenced by the significant stress change due to dyke intrusion. The related seismic activity along FF was characterized by some 50 minor shocks, one of which exceeded M3, apart from the mainshock.

Mt. Etna, the largest active onshore volcano in Europe, is a polygenetic basaltic volcano rising >3,300 m above s.l. in eastern Sicily. It started forming about 500 ka, at the outer edge of the Apennines-Maghrebides thrust belt (Branca, Coltelli, Groppelli, & Lentini, 2011; Lentini, Carbone, & Guarnieri, 2006) (Figure 1a). The present-day volcanic activity is characterized by frequent summit eruptions and occasional flank eruptions (Branca & Del Carlo, 2005), paired with frequent and diffuse volcano-tectonic seismicity consisting of low-magnitude events (M < 3) with shallow hypocentral depths (h < 5 km) (Alparone et al., 2015; Patanè, Cocina, Falsaperla, Privitera, & Spampinato, 2004). However, stronger earthquakes with magnitude up to ML ∼5 cause significant damage to the densely urbanized flanks of the volcano, representing a relevant source of hazard at a local scale (Azzaro, D'Amico, Peruzza, & Tuvè, 2013). Overall, local geodynamic processes at Mt. Etna are due to the interaction between regional tectonic stress, volcano dynamics (inflation due to magma uprising, dyke intrusions, etc.) and flank instability (Azzaro, Bonforte, Branca, & Gugliemino, 2013b and references therein; Ruch et al., 2013; Urlaub et al., 2018).

From the seismotectonic point of view, the most important fault system in the eastern flank of the volcano is the Timpe System (Figure 1b), that consists of a number of parallel east-facing faults with individual length up to 11 km and has generated the strongest

CONTACT Riccardo Civico riccardo.civico@ingv.it

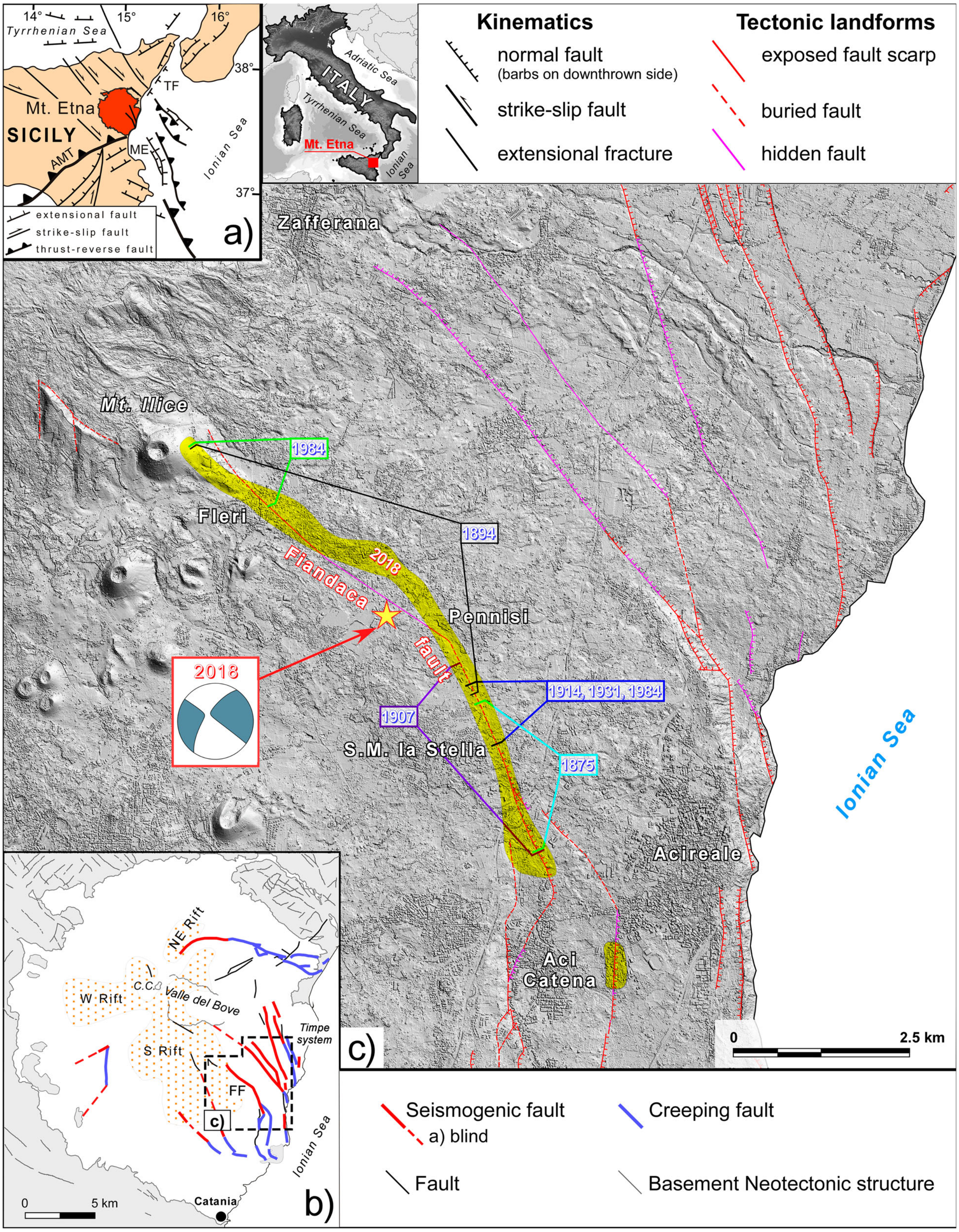

Figure 1. Tectonic setting of the study area. a) location map showing the Mt. Etna volcano in the framework of the Apennines-Maghrebian thrust-belt; b) sketch of the main active fault-systems on Mt. Etna (FF = Fiandaca Fault); c) detail of the Fiandaca Fault showing the extent of the 2018 surface faulting (yellow band), the focal mechanism of the 26 December 2018 earthquake and the historic surface faulting events.

earthquakes over the last 200 years (Azzaro, Branca, Gwinner, & Coltelli, 2012). These structures exhibit different fault behavior (Figure 1b), varying from purely stick-slip to stable creep, with slip rates ranging from 2 to 5 mm/yr. Extensive coseismic surface faulting during the historic period is well documented in this area, with complex mechanisms of rupture affecting the whole fault system (i.e. following a characteristic earthquake style) or individual segments (Azzaro, 1999).

The FF is a ~13 km-long late Quaternary fault featuring a transtensive dextral strike-slip kinematics (Figure 1). It is NNW-SSE oriented and turns in ~NS direction in its southern portion. Similar to nearby faults, its behavior varies along strike: fault creep affects the southern segment while seismogenic activity occurs along the central-northern sections. The 26 December 2018 mainshock entirely ruptured the locked section of the FF, as did the 1894 earthquakes (Figure 1c), whereas other historical events (1875, 1907, 1914, 1984 and 1997) produced faulting along shorter segments of the same structure (Azzaro, 1999). Reported displacements indicate prevailing right-lateral kinematics with a subordinate extensional component, and maximum coseismic slip in the order of 0.20 m.

Rapid and spatially dense collection of surface rupture data after an earthquake provides useful information for constraining the seismic source, in addition to support emergency response and ensure that coseismic slip is correctly measured without alteration due to weathering or road/infrastructure repairs as well as post-seismic slip. Therefore, the EMERGEO Working Group (prompt geological field survey team of the Istituto Nazionale di Geofisica e Vulcanologia) began surveying the coseismic surface effects within hours of the 26 December 2018 earthquake. The response of the EMERGEO Working Group was focused on the detailed recognition and mapping from field and aerial (drone) surveys of 1) the total extent of coseismic surface ruptures; 2) their geometric and kinematic characteristics; and 3) the coseismic surface slip distribution along the activated fault. The full dataset supporting points 2 and 3 is available at https://doi.pangaea.de/10.1594/PANGAEA.904332 and the related paper is currently submitted to *Scientific Data* (Villani et al., under review).

This paper represents a synthesis of the efforts of the EMERGEO Working Group to collect coseismic data on the 26 December ruptures. Here, we present a detailed and comprehensive report (Main Map) of the 26 December 2018 M_w 4.9 earthquake surface ruptures along the FF.

2. Methods

The survey was carried out according to the classical morphotectonic and structural geology methods, similarly to those adopted within the EMERGEO Working Group during the 2016 central Italy earthquake sequence (Civico et al., 2018; Villani et al., 2018). Our approach focused on a systematic survey of the epicentral area, mapping in detail the outcropping surface faulting, and measuring the strike of coseismic ruptures and displacement of both natural and cultural features. One of the main challenges in mapping the 26 December earthquake fault was to identify and locate the pattern of the primary rupture throughout a very densely urbanized area having limited access to private properties.

Field measurements were supported by the use of digital mobile devices equipped with specific software employing built-in GPS, magnetometer, and accelerometer (Rocklogger© mobile app, www.rockgecko.com), which allowed for quick and accurate structural data collection and real-time sharing (see details of the method in: EMERGEO Working Group, 2012 and Villani et al., 2018). In particular, the mobile devices were used to measure the position of the observation and the orientations of planes (dip angle, dip direction, strike) and lineations (rake, slip vector trend, slip vector plunge), as well as for taking georeferenced photos. Tapes, rulers, and rods were used for measuring length and offset of the ruptures (e.g. opening, strike-slip, vertical and net components). Strike measurements of ruptures with appreciable vertical separation were collected adopting the right hand rule (i.e. looking to the strike direction, the plane dips to the right of the observer). In addition, comprehensive mapping of the extent and the geometric characteristics of the surface ruptures at specific sites was also facilitated by Structure-from-Motion (SfM) photogrammetry (Westoby, Brasington, Glasser, Hambrey, & Reynolds, 2012), with images acquired during three separate drone flights.

The field dataset has been parsed and organized in a concise database consisting of nearly 900 georeferenced records (Villani et al., under review). Furthermore, a comprehensive photographic collection of the coseismic ruptures is available in EMERGEO Working Group, 2019.

On the basis of field measurements, the coseismic surface ruptures were traced on screen at up to 1:500 scale. The rupture traces are included in the Main Map as a line coverage with variable symbology depending on the different kinematics (see legend of Main Map). In detail, we define the following main kinematics: normal (opening $<$ 1 cm, throw $>$ 1 cm, strike-slip $<$ 1 cm or not available (n.a.)); hybrid (opening $>$1 cm, throw $>$ 1 cm, strike-slip n.a or $<$ 1 cm); tensional (opening $>$ 1 cm, throw $<$ 1 cm, strike-slip $<$ 1 cm or n.a.); transtensive (opening $\geq$ 1 cm, throw $>$ 1 cm, strike-slip $>$ 1 cm); strike-slip (opening $<$ 1 cm, throw $<$ 1 cm, strike-slip $>$ 1 cm); transpressive (opening $<$ 1 cm, throw $>$ 1 cm, strike-slip $>$ 1 cm); reverse (opening $<$ 1 cm, throw $>$ 1 cm, strike-slip $<$ 1 cm or n.a.); minor cracks (opening $<$ 1 cm, throw $<$ 1 cm, strike-slip $<$ 1 cm or n.a.). Uncertain and/or buried rupture traces are also included. Available slip vectors are reported as orange arrows along with the associated net offset values (indicating the net displacement of a coseismic rupture measured in centimetres along the slip vector, using piercing points). In order to depict the general spatial pattern of the surface offset, a selection of offset values (colour-coded as vertical, opening and strike-slip components) is also shown in the Main Map.

Rupture traces, slip vectors and offset values are drawn over a topographic base map built as a multi-layer of a) hillshaded relief from 2m-grid lidar-derived digital terrain model (available from Ministry of the Environment and for Protection of the Land and Sea – http://www.pcn.minambiente.it/), b) digital orthophoto flight 'ATA 2012–2013' from Regione Sicilia Web Map Service, and c) contour lines (10-m interval) from vectorial topographic maps at 1:10,000 scale (C.T.R. from Regione Sicilia). The Main Map is reduced at 1:10,000 scale, as this is the best compromise between the paper size, the extent of the study area and the desired map detail.

3. Results

The coseismic surface faulting associated with the 26 December 2018 earthquake (Figure 2) is mainly expressed by discrete rupture sets with lengths ranging from 0.5 m to a maximum of 530 m, mostly organized in sub-parallel strands with prevailing en-echelon left-stepping arrangement (Figure 2d), characterized by two prevailing peaks of strike at N340°-345° and N355°-360°, and by a subordinate trend of N335°-340°. The ruptures displaced different deposits (lavas, pyroclastics, and colluvium) as well as man-made features (Figure 2c,i,l) defining a principal deformation zone between a few meters to about 30-50 m wide (Figure 2h). The overall trend of the mapped ruptures follows the trace of the FF only in its southern section (between the villages of Pennisi and Aci Catena), whereas, it does not correspond with the northern section of the FF that was mapped on the basis of historical rupture information only (Azzaro et al., 2012). This section of the FF has been classified as a hidden fault, not having any clear long-term morphological expression but being revealed only by coseismic faulting effects (Azzaro, 1999).

The surface ruptures extended almost continuously along the FF for a length of about 8 km (Figure 1), whereas some other ruptures, with limited displacements, have been documented to the south along mapped and unknown faults, defining an overall rupture system of about 10 km (Figure 1 and Main Map). Among the various kinematics recognized in the field, nearly 50% of the ruptures are tensional open cracks, whereas about one third of the remaining ones display hybrid kinematics (a mixture of tensional and dip-slip) or are characterized by offset below the resolution of our measurements (indicated as minor cracks). Other ruptures display normal, reverse, strike-slip, transtensional or transpressive kinematics. Surface rupture displacements exhibit different values depending on the kinematics: the horizontal offset (strike slip) has a modal value of 0.08 m with a peak of 0.35 m; the throw has an average value of 0.1 m with a modal peak of 0.01 m; the opening has an average value of about 0.05 m, but local values as large as 2 m have been measured where gravitational sliding also occurred. The net slip (measured along the slip vectors) has an average value of about 0.09 m and a peak value of 0.35 m (Villani et al., under review).

4. Conclusions

Here we present the map of the surface ruptures following the 26 December 2016 Mw 4.9 Mt. Etna earthquake, the strongest event occurred in the area during the last 70 years. Soon after the event, we began surveying the coseismic effects at the surface, collecting geological and structural data to describe the ruptures geometry and kinematics.

Field data showed an almost continuous alignment of ground ruptures for an overall extent of about 8 km along the semi-hidden Fiandaca Fault (FF), belonging to the Timpe tectonic system in the eastern flank of the volcano. When minor ruptures along adjacent faults to the south are considered, the overall rupture length reaches about 10 km. Coseismic surface faulting was expressed mainly as discrete rupture sections with lengths ranging from 0.5 m to ca. 530 m, mostly organized in sub-parallel strands with prevailing en-echelon, left-stepping arrangement, defining a main deformation zone from a few meters to 30-50 m wide. The mapped ruptures are characterized in most cases by perceivable opening and by a dominant right-oblique sense of slip, with an average slip of about 0.09 m and a peak value of 0.35 m. It is also noteworthy that the ruptures vary significantly in their kinematic expression, denoting locally high degree of complexity of the surface faulting.

By providing a detailed picture of the coseismic ruptures at the surface based on a very dense dataset of field measurements (taken on average every ca. 10 m), this work helps in understanding in detail surface faulting at Etna as well as it represents an important contribution to the study of scaling relationships in volcano-tectonic domains (Azzaro et al., 2017; Nappi et al., 2018; Stirling, Goded, Berryman, & Litchfield, 2013; Wesnousky, 2008). Furthermore, it provides new data for implementing the community-sourced, worldwide database of surface ruptures associated with earthquakes (SUrface Rupture Earthquake (SURE) database – Baize et al., 2019), a basic tool to perform Probabilistic Fault Displacement Hazard Analysis (PFDHA).

5. Software

The field survey of the coseismic effects at the surface (type of observation, strike, vertical dislocation,

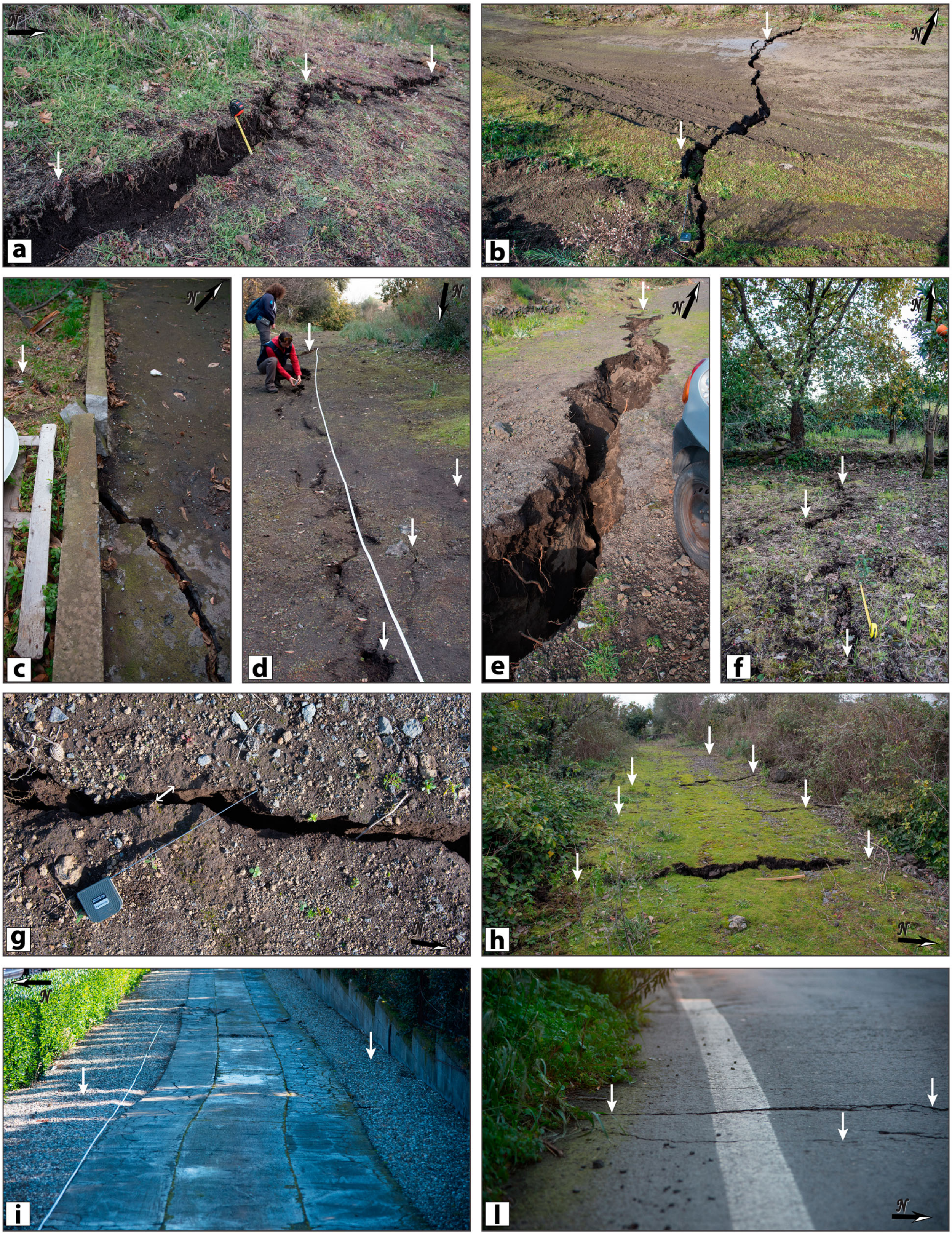

Figure 2. Examples of coseismic rupturesalong the Fiandaca Fault as seen in the field. Location of each picture is as follows: a) (37.6627 N, 15.0908 E); b) (37.6489 N, 15.1177 E) c) (37.6595 N, 15.0941 E); d) (37.6506 N, 15.1153 E); e) ((37.6465 N, 15.1225 E); f) (37.6426 N 15.1253 E); g) (37.6487 N, 15.1183 E); h) (37.6417 N, 15.1260 E); i) (37.6333 N, 15.1317 E); l) (37.6209 N, 15.1366 E).

opening, etc.) was performed using the Rocklogger© Android App for mobile devices. The data collected have been managed and stored in a georeferenced database using Esri ArcGIS Pro. Agisoft PhotoScan Professional has been used to derive high-resolution photomosaics from SfM image-based modeling. Adobe Illustrator CS6 was used for final map production.

Acknowledgments

Digital cartographic elements of the Carta Tecnica Regionale 1:10,000-scale by courtesy of Regione Sicilia. Hillshaded relief from 2m-grid lidar-derived digital terrain model by courtesy of Ministry of the Environment and for Protection of the Land and Sea - http://www.pcn.minambiente.it/ We thank local owners for having allowed the survey inside private properties. We thank Heike Apps, Jesse Kearse and F. Ramón Zúñiga for constructive comments that strengthened the manuscript. In addition, we thank Monica Pondrelli and Mike J. Smith for the editorial handling.

Disclosure statement

No potential conflict of interest was reported by the authors.

ORCID

Riccardo Civico http://orcid.org/0000-0002-5015-2155
Stefano Pucci http://orcid.org/0000-0002-3557-2936
Rosa Nappi http://orcid.org/0000-0002-1552-4398
Raffaele Azzaro http://orcid.org/0000-0001-8294-8687
Fabio Villani http://orcid.org/0000-0001-7133-0136
Daniela Pantosti http://orcid.org/0000-0001-7308-9104
Francesca R. Cinti http://orcid.org/0000-0003-1068-3223
Luca Pizzimenti http://orcid.org/0000-0003-1495-8175
Stefano Branca http://orcid.org/0000-0002-4971-4528
Carlo Alberto Brunori http://orcid.org/0000-0003-0862-8161
Marco Caciagli http://orcid.org/0000-0002-7248-4118
Luigi Cucci http://orcid.org/0000-0002-0238-2730
Salvatore D'amico http://orcid.org/0000-0003-0027-5381
Emanuela De Beni http://orcid.org/0000-0002-9867-1704
Paolo Marco De Martini http://orcid.org/0000-0002-3598-5191
Maria Teresa Mariucci http://orcid.org/0000-0002-5999-0446
Paola Montone http://orcid.org/0000-0002-9297-1730
Rosella Nave http://orcid.org/0000-0002-4091-9404
Tullio Ricci http://orcid.org/0000-0002-0553-5384
Vincenzo Sapia http://orcid.org/0000-0003-1958-2314
Alessandra Smedile http://orcid.org/0000-0002-2938-4816
Gabriele Tarabusi http://orcid.org/0000-0002-2497-6273
Roberto Vallone http://orcid.org/0000-0003-1208-9412
Alessandra Venuti http://orcid.org/0000-0002-0213-3355

References

Alparone, S., Maiolino, V., Mostaccio, A., Scaltrito, A., Ursino, A., Barberi, G., … Zuccarello, Z. (2015). Instrumental seismic catalogue of Mt. Etna earthquakes (Sicily, Italy): Ten years (2000-2010) of instrumental recordings. *Annals of Geophysics*, *58*(4), S0435. doi:10.4401/ag-65912015.

Azzaro, R. (1999). Earthquake surface faulting at Mount Etna volcano (Sicily) and implications for active tectonics. *Journal of Geodynamics*, *28*, 193–213.

Azzaro, R., Barberi, G., D'Amico, S., Pace, B., Peruzza, L., & Tuvè, T. (2017). When probabilistic seismic hazard climbs volcanoes: The Mt. Etna case, Italy – part 1: Model components for sources parameterization. *Natural Hazards and Earth System Sciences*, *17*, 1981–1998. doi:10.5194/nhess-17-1981-2017

Azzaro, R., Bonforte, A., Branca, S., & Gugliemino, F. (2013b). Geometry and kinematics of the fault systems controlling the unstable flank of Etna volcano (Sicily). *Journal of Volcanology and Geothermal Research*, *251*, 5–15. doi:10.1016/j.jvolgeores.2012.10.001

Azzaro, R., Branca, S., Gwinner, K., & Coltelli, M. (2012). The volcano-tectonic map of Etna volcano, 1:100.000 scale: Morphotectonic analysis from high-resolution DEM integrated with geologic, active faulting and seismotectonic data. *Italian Journal of Geosciences (Boll. Soc. Geol. It.)*, *131*(1), 153–170.

Azzaro, R., D'Amico, S., Peruzza, L., & Tuvè, T. (2013). Probabilistic seismic hazard at Mt. Etna (Italy): the contribution of local fault activity in mid-term assessment. *Journal of Volcanology and Geothermal Research*, *251*, 158–169.

Baize, S., Nurminen, F., Sarmiento, A., Dawson, T., Takao, M., Scotti, O., … Villamor, P. (2019). A worldwide and Unified database of surface ruptures 1 (SURE) for fault displacement hazard Analyses. *Seismological Research Letters*, doi:10.1785/0220190144

Bonforte, A., Guglielmino, F., & Puglisi, G. (2019). Large dyke intrusion and small eruption: The December 24, 2018 Mt. Etna eruption imaged by Sentinel-1 data (2019). *Terra Nova*, *00*, 1–8. doi:10.1111/ter.12403

Branca, S., Coltelli, M., Groppelli, G., & Lentini, F. (2011). Geological map of Etna volcano, 1:50,000 scale. *Italian Journal of Geosciences (Boll. Soc. Geol. It.)*, *130*(3), 265–291.

Branca, S., & Del Carlo, P. (2005). Types of eruptions of Etna volcano AD 1670-2003: Implications for short-term eruptive behaviour. *Bulletin of Volcanology*, *67*, 732–742.

Civico, R., Pucci, S., Villani, F., Pizzimenti, L., De Martini, P. M., Nappi, R., & the Open EMERGEO Working Group. (2018). Surface ruptures following the 30 October 2016 Mw 6.5 Norcia earthquake, central Italy. *Journal of Maps*, doi:10.1080/17445647.2018.1441756

De Novellis, V., Atzori, S., De Luca, C., Manzo, M., Valerio, E., Bonano, M., et al. (2019). DInSAR analysis and analytical modeling of Mount Etna displacements: The December 2018 volcano-tectonic crisis. *Geophysical Research Letters*, *46*. doi:10.1029/2019GL082467

EMERGEO Working Group. (2012). Technologies and new approaches used by the INGV EMERGEO Working Group for real time data sourcing and processing during the Emilia Romagna (northern Italy) 2012 earthquake sequence. *Annals of Geophysics*, *55*(4), doi:10.4401/ag-6117

EMERGEO Working Group. (2019). Photographic collection of the coseismic geological effects originated by the 26th December 2018 Etna (Sicily) earthquake. *Miscellaneous INGV*, *48*, 176. Retrieved from http://editoria.rm.ingv.it/miscellanea/2019/miscellanea48/

Lentini, F., Carbone, S., & Guarnieri, P. (2006). Collisional and postcollisional tectonics of the Apenninic–Maghrebian orogen (southern Italy). In Y. Dilek, & S. Pavlides (Eds.), *Postcollisional Tectonics and Magmatism in the mediterranean region and Asia. The geological society of America, Special Papers, 409* (pp. 57–81). Boulder: Geological Society of America.

Nappi, R., Alessio, G., Gaudiosi, G., Nave, R., Marotta, E., Siniscalchi, V., … Porfido, S. (2018). The 21 August 2017 MD 4.0 Casamicciola earthquake: First evidence of coseismic normal surface faulting at the Ischia volcanic Island. *Seismological Research Letters*, *89*(4), 1323–1334.

Patanè, D., Cocina, O., Falsaperla, S., Privitera, E., & Spampinato, S. (2004). Mt. Etna Volcano: A Seismological

Framework. In A. Bonaccorso, S. Calvari, M. Coltelli, C. Del Negro, & S. Falsaperla (Eds.), *Mt. Etna: Volcano Laboratory*. American Geophysical Union. doi:10.1029/143GM10

QUEST Working Group. (2019). Il terremoto etneo del 26 dicembre 2018, Mw4.9: rilievo degli effetti macrosismici. Report INGV n. 1 del 06/02/2019, pp. 9. doi:10.5281/zenodo.2558168. http://www.questingv.it/index.php/rilievi-macrosismici/36-etna-26-12-2018-mw-4-9/file

Ruch, J., Pepe, S., Casu, F., Solaro, G., Pepe, A., Acocella, V., … Sansosti, E. (2013). Seismo-tectonic behavior of the Pernicana fault system (Mt Etna): A gauge for volcano flank instability? *Journal of Geophysical Research: Solid Earth*, *118*, 4398–4409. doi:10.1002/jgrb.50281

Stirling, M., Goded, T., Berryman, K., & Litchfield, N. (2013). Selection of earthquake scaling relationships for seismic-hazard analysis. *Bulletin of the Seismological Society of America*, *103*(6), 2993–3011. doi:10.1785/0120130052

Urlaub, M., Petersen, F., Gross, F., Bonforte, A., Puglisi, G., Guglielmino, F., … Kopp, H. (2018). Gravitational collapse of Mount Etna's southeastern flank. *Science Advances*, *4*(10), eaat9700. doi:10.1126/sciadv.aat9700

Villani, F., Civico, R., Pucci, S., Pizzimenti, L., Nappi, R., De Martini, P. M. & The Open EMERGEO Working Group (2018). A database of the coseismic effects following the 30 October 2016 Norcia earthquake in Central Italy. *Scientific Data*, doi:10.1038/sdata.2018.49

Villani, F., Pucci, S., Azzaro, R., Civico, R., Cinti, F. R., Pizzimenti, L., … Venuti, A. (submitted). Surface ruptures database related to the 26 December 2018, MW 4.9 Mt. Etna earthquake (southern Italy). Submitted to Scientific Data.

Wesnousky, S. G. (2008). Displacement and geometrical characteristics of earthquake surface ruptures: Issues and implications for seismic-hazard analysis and the process of earthquake rupture. *Bulletin of the Seismological Society of America*, *98*(4), 1609–1632. doi:10.1785/0120070111

Westoby, M. J., Brasington, J., Glasser, N. F., Hambrey, M. J., & Reynolds, J. M. (2012). 'Structure-from-Motion' photogrammetry: A low-cost, effective tool for geoscience applications. *Geomorphology*, *179*, 300–314. doi:10.1016/j.geomorph.2012.08.021